Neuromorphological Phenotyping in Transgenic Mice: A Multiscale Fractal Analysis

Andreas Schierwagen[1], Luciano da Fontoura Costa[2],
Alan Alpar[3], Ulrich G¨artner[3],
and Thomas Arendt[3]

[1]Institute for Computer Science, University of Leipzig, 04109 Leipzig, Germany;
schierwa@informatik.uni-leipzig.de
[2]Institute of Physics at S˜ao Carlos, University of S˜ao Paulo, Caixa Postal 369, 13560-970 S˜ao Carlos, SP, Brazil
[3]Department of Neuroanatomy, Paul Flechsig Institute for Brain Research, University of Leipzig, 04109 Leipzig, Germany

In: **Mathematical Modeling of Biological Systems, Volume II.**

A. Deutsch, R. Bravo de la Parra, R. de Boer, O. Diekmann, P. Jagers, E. Kisdi, M. Kretzschmar, P. Lansky and H. Metz (eds).

Birkhäuser, Boston, 191-199 (2007)

16

Neuromorphological Phenotyping in Transgenic Mice: A Multiscale Fractal Analysis

Andreas Schierwagen,[1] Luciano da Fontoura Costa,[2] Alan Alpar,[3] Ulrich Gärtner,[3] and Thomas Arendt[3]

[1] Institute for Computer Science, University of Leipzig, 04109 Leipzig, Germany; schierwa@informatik.uni-leipzig.de
[2] Institute of Physics at São Carlos, University of São Paulo, Caixa Postal 369, 13560-970 São Carlos, SP, Brazil
[3] Department of Neuroanatomy, Paul Flechsig Institute for Brain Research, University of Leipzig, 04109 Leipzig, Germany

Summary. 3D morphological data have been used to quantitatively characterize the morphological phenotype of pyramidal neurons in transgenic mice. We calculated the multiscale fractal dimension (MFD) of reconstructed neuronal cells. Changes in the complexity of neuronal morphology due to permanent activation of p21Ras in the primary somatosensory cortex of transgenic mice correlate with changes in the MFD of dendrites of pyramidal neurons. Transgenic neurons seem slightly less complex (i.e., have lower peak fractal dimension) if compared with the wild type. On the other hand, the enhanced p21Ras activity in transgenic mice may lead to greater variety of the cell morphological phenotype.

Key words: Local fractal dimension, multiscale fractal analysis, pyramidal neurons, dendritic morphology, somatosensory cortex, mouse, phenotyping.

16.1 Introduction

Transgenic mice mutations provide important means for understanding gene function, as well as for developing therapies for genetic diseases. In these mutants, the gene overexpression may affect several organs and tissues, including the brain. In a specific mouse mutant introduced by [8] a permanently active Ras protein (p21 H-ras^{Val12}). in post-mitotic neurons is expressed. Enhanced p21Ras activity results in a dramatically enlarged dendritic tree. In both cortical layers II/III and V, the total surface area and the total volume of dendritic trees is greatly increased. This is mainly caused by increased dendritic diameter and tree degree [1].

The aim of this chapter is to provide further evidence for these findings. For this, quantitative aspects of dendritic tree shape have been analyzed. There are several methods for describing trees by quantitative measures. Neurons are three-dimensional (3D) objects, and the location of their somata within the nervous tissue, as well as the number, spatial dimensioning, branching complexity and 3D embedding of their axonal

and dendritic trees are salient shape characteristics that may significantly distinguish between different cell types.

The branching complexity of neuronal arborizations is determined both by topological and metrical properties (cf. [9]). For topological characterization, a neuronal tree is reduced to a skeleton structure of points (branching or terminal points) and segments between these points. Such a skeleton forms a typical rooted tree out of a finite set of possible different tree types. Dendritic segments can be labeled by centrifugal order (number of segments on the path to the root). Metrical aspects include length and diameter of the segments, path lengths (total length of the path from the dendritic root to a branch point or terminal tip), radial distances of terminal tips from the center of the cell and branching angles. Further details include measures for the irregularity, spatial orientation and curvature of the branches.

Another class of measures is related to the spatial embedding in 3D space, as characterized by the spatial dimensioning, spatial density, spatial orientation and space filling of the structure. In this study, the focus is on space filling or fractal aspects of dendritic tree shape. There are several methods for describing trees by fractal dimensions (see [10, 11] for early fractal analyses of neuronal dendritic trees, and, e.g., [6] for a review).

Multiscale (or *local*) fractal analysis [3, 4, 7] has been demonstrated to be an effective means for characterization of neuronal complexity. This type of analysis seems to be particularly suitable in the present case because the multiscale fractal dimension is independent of size-related parameters like surface area and volume. The aim of this study is to show that observed changes in the complexity of neuronal morphology due to transgenic activation of p21Ras in the primary somatosensory cortex of mice correlate with changes in the multiscale fractal dimensions of dendrites of pyramidal neurons.

16.2 Materials and Methods

Two sets of pyramidal neurons (17 cells from wild type and 26 cells from transgenic mice) were reconstructed and digitized using Neurolucida (MicroBrightField, Inc.) as described elsewhere [1]. The morphology files created with Neurolucida were processed with CVAPP [2], a freely available program for cell viewing, editing and format converting (Fig. 16.1). Images were thresholded resulting in binary images with 1- and 0-voxels representing the neuron shape and background regions, respectively. Therefore, in digitized 3D binary images, the shape of a neuron is represented by the set of 1-voxels.

The binary images of the neuron shape patterns were used for calculating the multiscale fractal dimension (MFD), a measure related to the image complexity [4, 7]. It is computed through the Minkowski sausage approach, which can be described as follows: Let the neuron shape under study be represented by the set S of the Cartesian coordinates of each of its 1-voxels. Its exact dilation by a radius r is defined as the union of all spheres of radius r centered at each of the elements of S. A series of dila-

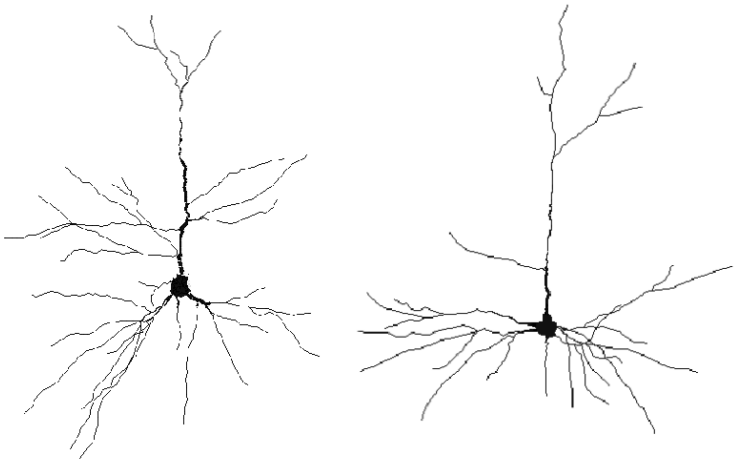

Fig. 16.1. Pyramidal cells rendered with CVAPP. Displayed are one example each of transgenic (cell SE15, left) and wild type neurons (cell WT17, right).

tions on the image is made, with radii r_i equivalent to the intrinsic lattice distances, the so-called exact distances. At each dilation, the volume $V(r_i)$ of the image is computed.

The volume $V(r)$ of the shape S is therefore defined by

$$V(r) = \sum_{i=1}^{M} V(r_i)\,\delta(r - r_i), \tag{16.1}$$

where $\delta(.)$ is the Dirac delta function and M is the index of the largest exact distance being considered. As $V(r)$ is a discontinuous function on r, which is a consequence of the discrete nature of r_i, it is necessary to interpolate between the Dirac deltas, which is here accomplished by convolving $V(r)$ with the Gaussian $g_\sigma(r) = 1/\sigma/\sqrt{2\pi}\,\exp(-0.5(r/\sigma)^2)$, yielding the following interpolated volume:

$$v_\sigma(r) = \sum_{i=1}^{M} V(r_i) g_\sigma(r - r_i). \tag{16.2}$$

It is important to choose a suitable value of the standard deviation parameter, σ, that is large enough just to interpolate between the largest gaps between the exact radii, which occur for small values of r. The cumulative volume is defined as

$$C(s) = \int_{-\infty}^{s} v_\sigma(r)\,dr. \tag{16.3}$$

The Euclidean distance is now represented in terms of its logarithm, leading to the spatial scale parameter $s = \log(r)$, so that the exact radii are expressed as $s_i = \log(r_i)$. The MFD $f(s)$ of the set S of voxel elements can be defined then by

$$f(s) = 3 - \frac{d}{ds}\log(C(s)) = 3 - \frac{C'(s)}{C(s)}. \tag{16.4}$$

While the traditional fractal dimension corresponds to a single scalar value, the MFD becomes a function of the spatial scale parameter s, providing additional information about the analyzed shapes. Among others, the following measurements quantify meaningful features of the MFD curve: peak fractality, f_M (the maximum value along the MFD curve), characteristic scale, s_M (the value of the spatial scale for which f_M is obtained) and average fractality, $\langle f \rangle$. For the computational implementation of this method, see [4].

16.3 Results

In Fig. 16.2, an example calculation of the MFD curve for the transgenic cell SE8 is shown. Following the scheme defined in Equations 16.1–16.4, the MFD depending on s eventually was obtained. As shown there, the fractal dimension decreases at both micro and macro scales, and the peak fractal dimension value, f_M, is observed at an intermediate scale value, s_M. This behavior is caused by the finite size of neuron images (see Section 16.4).

The sample histograms of the three parameters utilized, f_M, s_M and $\langle f \rangle$, are presented in Fig. 16.3. For f_M, a bimodal distribution for the transgenic cases results, while wild type cells produced a single mode (Fig. 16.3, top). The distribution of the characteristic scales s_M observed suggests that the two types of cells are characterized by similar values of this parameter (Fig. 16.3, middle). Finally, the distributions of $\langle f \rangle$ are bimodal in the case of transgenic cells, and unimodal for wild type cells (Fig. 16.3, bottom).

The scatterplots in Fig. 16.4 depict the mutual relationships between f_M, s_M and

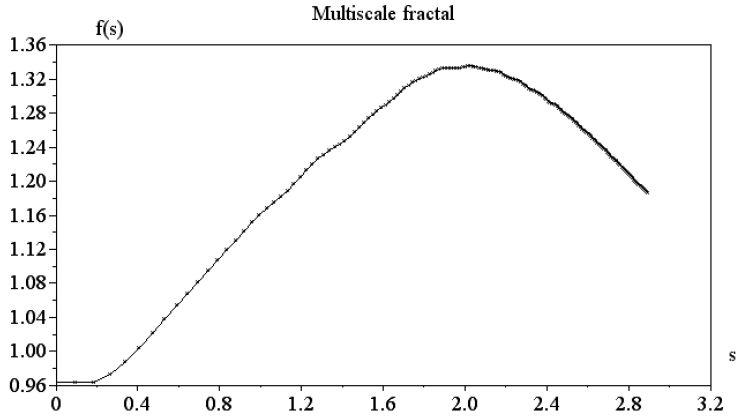

Fig. 16.2. Example calculation of MFD for transgenic cell SE8. Shown is the MFD in terms of s. See text for details.

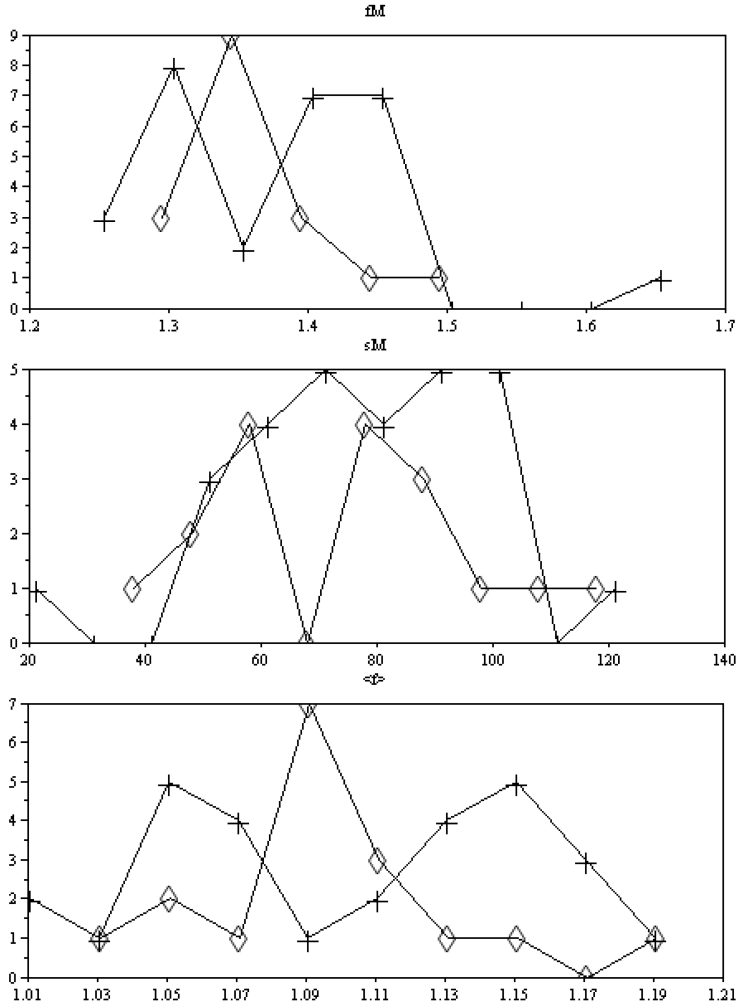

Fig. 16.3. Histograms of the three parameters calculated. Presented are numbers of occurrence (ordinate) of peak fractal dimension, f_M, characteristic scale, s_M, and average fractal dimension, $\langle f \rangle$. Wild type and transgenic cases are identified by diamonds and crosses, respectively.

$\langle f \rangle$. The strong correlation between peak fractal dimension, f_M, and maximum fractality scale, s_M, is obvious.

Fig. 16.5 presents Gaussian densities after principal component analysis for the feature combinations (f_M, s_M) and (f_M, $\langle f \rangle$), after normal statistical transformation (leading to null mean and unit variance in both cases). By the strong correlation between f_M and s_M (Fig. 16.4) the first principal component explains most of the variance and is usable as the measure of complexity. Thus, the feature combination (f_M, s_M) enables the separation of the two cell types. As indicated in Fig. 16.5, transgenic

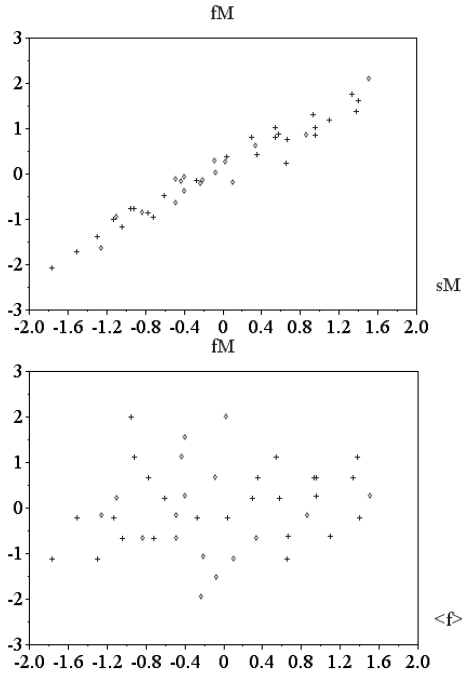

Fig. 16.4. Scatterplots of f_M versus s_M (top) and f_M versus $\langle f \rangle$ (bottom). The meaning of symbols is as in Fig. 16.3.

tend to be less complex as they have a lower fractality, expressing at the same time greater variance.

16.4 Discussion

In this chapter 3D data on neuronal morphology has been used to quantitatively characterize the phenotype of transgenic neurons. We calculated the local/multiscale fractal dimension (MFD) of neuronal cells reconstructed in 3D. It is known that the fractality of objects in nature is limited and varies along the spatial scales. On one hand, this is due to the finite size of any real object, leading to behavior close to that of a point for spatial scales much larger than the object diameter. On the other hand, structural properties are usually different at smaller spatial scales. For instance, a cauliflower or a fern has fractal properties only over two or three hierarchical levels, with a smoother characteristic at smaller scales. Moreover, the limited resolution of the image acquisition devices imposes further constraints on the fractal behavior at small spatial scales. The MFD approach explicitly points to this fact.

The advantages of the MFD (a function of the spatial scale) over the traditional fractal dimension (a single scalar value) reside in providing additional information about the analyzed shapes. Thus, we computed complementary features such as the

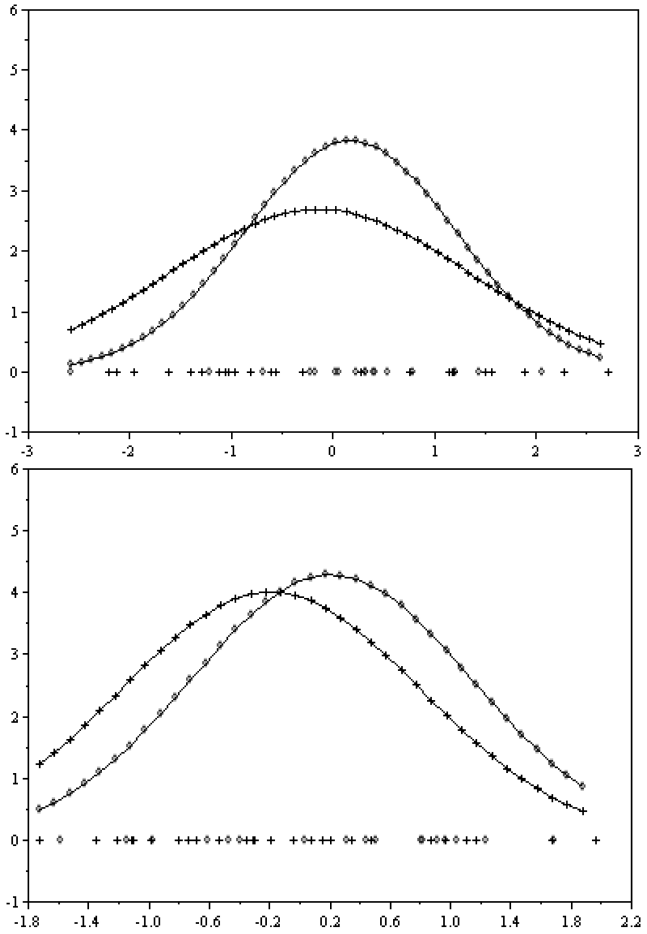

Fig. 16.5. Gaussian densities after principal component analysis for (f_M, s_M) (top) and $(f_M, \langle f \rangle)$ (bottom). The meaning of symbols is as in Fig. 16.3.

peak fractality, the characteristic scale where it occurs and the average fractality, for quantifying and characterizing the cell types. Two sets of neurons, i.e., pyramidal cells from wild type and p21 H-ras$^{\text{Val12}}$ transgenic mice, have been analyzed. The results obtained after principal component analysis show that transgenic neurons are slightly less complex, as measured by the peak fractal dimension, f_M, if compared to their wild type counterpart, while the other two features considered (maximum fractality scale, s_M, and average fractal dimension, $\langle f \rangle$) did not reveal differences between the two types. Transgenic pyramidal neurons are characterized by increased dispersion if compared to the wild type pyramidal neurons, suggesting that the enhanced p21Ras activity in transgenic mice may lead to greater variety of the cell morphological phenotype.

These findings have recently been substantiated by a percolation analysis accomplished with the same data set. The percolation transform [5] is particularly useful for the characterization of spatial density of distributed points, and it represents an alternative to the multiscale fractal analysis reported here. As the latter, the percolation analysis is independent of size-related parameters like area and volume of the neuronal cells. We were able to verify that changes in the global character of the percolation transform curves derived from the reference points (i.e., dendritic tips and branch points) of the dendrites of pyramidal neurons correlate with changes in the complexity of neuronal morphology due to the activation of p21Ras in the primary somatosensory cortex of transgenic mice.

Acknowledgments

This study was partly supported by Deutsche Forschungsgemeinschaft (grant GA716/1-1), FAPESP and CNPq.

References

1. Alpar, A., Palm, K., Schierwagen, A., Arendt, T., Gärtner, U.: Expression of constitutively active p21H-rasVal12 in postmitotic pyramidal neurons results in increased dendritic size and complexity. J. Comp. Neurol., **467**, 119–133 (2003).
2. Cannon, R.C.: Structure editing and conversion with CVAPP (2000). http://www.compneuro.org/CDROM/nmorph/usage.htmlMonographs
3. Costa, L.F., Cesar, R. Jr.: Shape Analysis and Classification: Theory and Practice. CRC Press, Boca Raton, FL (2001)
4. Costa, L.F., Manoel, E.T.M., Faucereau, F., Chelly, J., van Pelt, J., Ramakers, G.J.A.: A shape analysis framework for neuromorphometry. Network: Comput. Neural Syst., **13**, 283–310 (2002).
5. Costa, L.F., Barbosa, M.S., Schierwagen, A., Alpár, A., Gärtner, U., Arendt, T.: Active percolation analysis of pyramidal neurons of somatosensory cortex: A comparison of wild type and p21H-rasVal12 transgenic mice. Int. J. Mod. Phys. C, **16**, 655–667 (2005).
6. Fernandez, E., Jelinek, H.F.: Use of fractal theory in neuroscience: Methods, advantages, and potential problems. Methods, **24**, 309–321 (2001).
7. Havlin, S., Ben-Avraham, D.: Fractal dimensionality of polymer chains. J. Phys. A: Math. Gen., **15**, L311–L316 (1982).
8. Heumann, R., Goemans, Ch., Bartsch, D., Lingenhöhl, K., Waldmeier, P.C., Hengerer, B., Allegrini, P.R., Schellander, K., Wagner, E.F., Arendt, Th., Kamdem, R.H., Obst-Pernberg, K., Narz, F., Wahle, P., Berns, H.: Constitutive activation of Ras in neurons promotes hypertrophy and protects from lesion-induced degeneration. J. Cell Biol., **151**, 1537–1548 (2000).
9. Van Pelt, J., Schierwagen, A.: Morphological analysis and modeling of neuronal dendrites. Math. Biosciences, **188**, 147–155 (2004).
10. Schierwagen, A.: Dendritic branching patterns. In: Degn, H., Holden, A.V., Olsen, L.F. (eds) *Chaos in Biological Systems*. Plenum Press, New York and London, 191–193 (1987).
11. Schierwagen, A.: Scale-invariant diffusive growth: A dissipative principle relating neuronal form to function. In: Maynard-Smith, J., Vida, G. (eds) *Organizational Constraints on the Dynamics of Evolution*. Manchester University Press, Manchester, 167–189 (1990).